ABOUT THE DIFFERENCE IN THE QUADRUPOLE SPLITTING OF WATER BETWEEN CATIONIC AND ANIONIC NEMATIC LYOTROPIC LIQUID CRYSTALS. ^{2}H-NMR AND MOLECULAR DYNAMICS STUDY

*H. AHUMADA[1], R. MONTECINOS[1], R. MARTINEZ[2], R. ARAYA-MATURANA[3] AND B. WEISS-LÓPEZ[1]**

[1] Departamento de Química, Facultad de Ciencias, Universidad de Chile, Santiago, Chile

[2]Departamento de Ciencias Químicas, Facultad de Ecología y Recursos Naturales Universidad Andrés Bello, República 275, Santiago, Chile.

[3] Departamento de Química Orgánica y Fisicoquímica, Facultad de Ciencias Químicas y Farmacéuticas, Universidad de Chile, Santiago 1, Chile.

Keywords: ^{2}H-NMR, Discotic Nematic Lyomesophases, Molecular Dynamics.

ABSTRACT

Deuterium quadrupole splittings, of deuterated water, $\Delta\nu$, in anionic discotic nematic lyomesophases are always much larger than in cationic mesophases. To explore the possible origins of this difference, $\Delta\nu$ and T_1 relaxation times of HDO (H_2O 0.2% D_2O) and decanol (DeOH 14% α-d_2), in solutions of cationic and anionic discotic lyotropic nematic liquid crystals, were measured using ^{2}H-NMR. The four component mesophases were prepared based on tetradecyltrimethylammonium bromide, (TTAB/DeOH/NaBr/H_2O), and cesium N-dodecanoyl-L-alaninate, (CsDAla/DeOH/KCl/H_2O), amphiphiles with cationic and anionic head-groups, respectively. For a better understanding of the experimental results, 15 ns molecular dynamics (MD) trajectories of both systems were calculated. The results suggest that the large difference observed in the quadrupole splittings of the solvent can be mainly attributed to a preferential orientation of the water molecules, induced by the strong electric field generated by the electrical bilayer formed at the interface of the anionic mesophase. Restrictions to solvent reorientational dynamics or differences in the thickness of the interface do not seem to play a significant role to explain the observed difference.

INTRODUCTION

The study of the interactions among the different components of molecular assemblies, such as micelles, vesicles, bilayers, lyotropic liquid crystals and others, is a topic of current research interest.[1-5] In particular, interactions between the solvent and head-groups have received special attention. A common feature to most of these systems is that they are made of amphiphilic molecules usually dissolved in water. In general, they present at least three different regions of interest: (a) the aqueous phase, containing the counter ions and other dissolved molecules or ions, (b) the interface, formed by the head groups, ions and solvent, and (c) the hydrophobic region, made of the hydrocarbon tails. The limits between these regions have not been uniquely defined. For instance, in phospholipid bilayers the interface has been defined as the region where the water density decreases from 90% to 10% the bulk density, moving along the normal to the surface.[6]

Perhaps the most interesting region present in all these molecular aggregates is the interface. With a significant charge density, the very strong electrostatic interactions present in this region are going to play a central role in the stabilization of the aggregate. This is particularly important for discotic nematic lyotropic liquid crystals, where the charged head groups are significantly close to each other due to the flat surface. Moreover, the type of interactions between the solvent molecules and the head-groups seems to be very important in determining the type of phase that is going to be formed.[7]

It has been observed that the quadrupole splitting of HDO in nematic discotic anionic lyotropic liquid crystals is several times bigger than the value observed in cationic mesophases. For example, in cationic liquid crystals made of hexadecylpyridinium chloride and TTAB, the splittings are between 30 Hz and 70 Hz for the former and between 15 Hz and 25 Hz for the later.[8,9] On the other hand, mesophases prepared with sodium and cesium decylsulphate show much larger HDO splittings, about 442 Hz and 226 Hz respectively.[10,11] Anionic cholesteric discotic nematic lyomesophases, based on cesium and potassium N-dodecanoyl-L-alaninate, also display large HDO quadrupole splittings, about 180 Hz and 420 Hz, respectively.[12,13] All these values, in cationic as well as anionic mesophases, are moderately dependent on the nature and concentration of decanol, the guest molecules and/or ions added to the solution.

The origin of the observed differences may be attributed to at least three different reasons: (1) the thickness of the anionic interfaces is always significantly bigger than in cationic interfaces, enclosing a larger amount of water; (2) the water at the anionic interface has significantly slower mobility; (3) there is a preferential orientation of the interstitial water in the anionic interface as compared to the cationic one. In the cationic mesophase the solvent should be rotating more randomly. In this situation, the mobility of DHO in terms of the value of the rotational correlation time should not be necessarily significantly different.

In this work we present an experimental (^{2}H-NMR) and theoretical (MD) study to explore the origins of the large observed differences between the solvent quadrupole splitting of these lyomesophases. For this purpose, we have measured the ^{2}H-NMR quadrupole splittings and longitudinal relaxation times of DHO and DeOH-α-d_2 in cationic and anionic lyomesophases prepared from TTAB and CsDAla. For a better understanding of the experimental results, 15 ns Molecular Dynamics trajectory calculations of both systems, represented as bilayers, were performed.

EXPERIMENTAL

Mesophase Preparations

TTAB was obtained from commercial sources and crystallized several times before use. The liquid crystal solution was prepared by dissolving 0.210 g of TTAB, 0.100 g of NaBr and 38 µl of DeOH in 0.50 ml of H_2O (0.2% D_2O). The composition employed in this work was very similar to previously reported lyomesophases prepared with TTAB.[8,9]

The cholesteric mesophase was prepared by dissolving 0.264 g of CsDAla, 0.025 g of KCl and 60 µl of DeOH (14%-α-d_2) in 0.48 ml of H_2O (0.2% D_2O). The synthesis of CsDAla and the composition of the sample were obtained from previous work.[12]

NMR Spectra. NMR spectra were recorded at 300K using a Bruker AVANCE-400 spectrometer in the Centro de Servicios Externos, at the Pontificia Universidad Católica de Chile. Proton spectra were obtained at 400MHz from the ^1H channel of a broadband probe and ^2H spectra were obtained at 61.4 MHz using the X channel of the same probe. A 30 kHz spectral window and 16 kB file size was employed. Relaxation times were obtained with the inversion recovery experiment, implemented in the instrument's software, with a ^2H 90° pulse length of 19 µs. The experimental errors in the measured quadrupole splittings were estimated to be ±2 Hz for HDO and ±10 Hz for DeOH, and the errors in the relaxation times were estimated to be ±5 ms for HDO and ±15 ms for DeOH.

Molecular Dynamics. Except for the structures of TTA^+, $DAla^-$ ions and decanol, for which a molecular editor was employed, all bilayer setup, trajectory calculations and analysis were performed using the GROMACS v 3.0 software package.[14] For the visualization of the trajectories and molecular graphics the VMD[15] program was used. The solvent was simulated at atomistic level using a previously described model.[16]

The force field employed in both cases was a mixture of GROMOS[17,18] and that of Bergier et al.[19] Since the potential field does not include parameters for cesium and bromide, the parameters for cesium were transferred from the OPLS force field[20-26] and instead of bromide we used chloride. The united atom approximation was employed for the hydrogen atoms in the aliphatic chains. The charges of $TDTMA^+$, $DAla^-$ and DeOH were obtained from 6-31G* ab-initio full geometry optimization calculations. The Ryckaert-Bellemans potential function[27] was used to calculate the contribution to the potential of the aliphatic chain torsions. LINCS[28] was used to constrain the bond lengths of the surfactant chains and SETTLE[29] to restrict the structure of the water molecules. Long range electrostatic interactions were calculated using PME,[30,31] with a 1nm cut-off. The update of the neighbor list was performed every 10 time steps. A 1nm cut-off was used for the Lennard-Jones potential. To maintain the temperature constant at 300 K (water, salt and surfactants coupled independently to the bath) and the pressure at a value of 1 bar, we have used Berendsen's weak coupling algorithm,[32] with time constants of 0.1 ps and 1 ps for T and P, respectively. The time step size in both simulations was 2 fs. All the calculations were made using a cluster of 22 Pentium III 1-GHz processors.

RESULTS AND DISCUSSION

NMR. Figure 1 shows the ^2H-NMR T_1IR experiment for the measurement of the longitudinal spin relaxation times, T_1, of HDO and DeOH-α-d_2 in the CsDAla mesophase.

Table 1 shows the values of T_1 obtained from the exponential recovery adjustment and the values of the quadrupole splittings, Δν, which can be measured directly from the spectrum in both mesophases. Δν and T_1 of HDO are functions of the interactions of the solvent at the interface. From Table 1 it is seen that the quadrupole splitting of HDO in TTAB is more than 15 times smaller than the splitting observed in CsDAla; however, the longitudinal relaxation time is only about 30% smaller. Besides, Δν of DeOH and HDO seem to correlate better in both mesophases, as usually seen.[8-12] Δν of DeOH is a function of the internal dynamics and the size of the aggregate.

Table 1. Deuterium quadrupole splittings, Δν (Hz) and longitudinal relaxation times, T_1 (ms), of HDO and DeOH in TTAC and CsDAla discotic nematic lyomesophases. Estimated errors are given in the text.

	TTAB		CsDAla	
	HDO	DeOH	HDO	DeOH
Δν	15	17456	230	12750
T_1	240	90	328	72

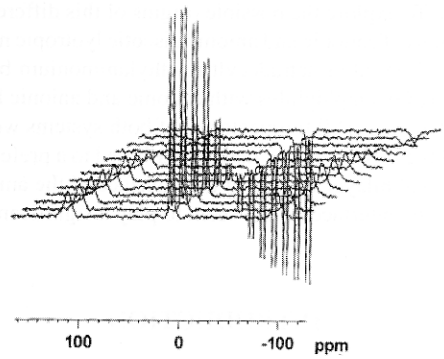

Fig. 1. Inversion recovery experiment to determine T_1 of HDO and DeOH in CsDAla mesophase. The quadrupole splittings can be measured directly from the spectrum.

Quadrupole splittings are composite properties, i.e. the observed value depends on two variables: (1) the average orientation of the electric field gradient, experienced by the nucleus, with respect to the magnetic field direction, and (2) the dynamics of the gradient around that average, the so called reorientational dynamics. An experimentally determined quadrupole splitting, obtained from the NMR spectrum of anisotropic solutions or solids, is closely related to the order parameter of the principal axis of the electric field gradient. They are residual properties in the sense that the observed values are always smaller than the value measured in oriented solid state samples. Order parameters can have values ranging from -0.5 for an axis oriented perpendicular to the magnetic field, to +1 for an axis parallel to the field. The value 0 can arise from an axis oriented at the magic angle or a randomly rotating axis, like a small molecule in isotropic low viscosity solutions.

Longitudinal magnetic relaxation of nuclei with spin ≥1 is strongly dominated by the quadrupolar interaction, which couples the electric quadrupole moment of the nucleus to the electric field gradient that it experiences from the electron density. Assuming that the rotational autocorrelation function of the gradient vector can be represented by an exponential first order decay, T_1 depends on the rotational correlation time according to:[33]

$$1/T_1 = (3/80)\,(1+\eta^2/3)\,[(2\pi eQ/h)(\partial^2V/\partial z^2)]^2\,\{J(\omega_o)+4J(2\omega_o)\}$$

$$J(\omega_o) = 2\tau_c / (1 + \omega_o{}^2\tau_c{}^2)$$

$$J(2\omega_o) = 2\tau_c / (1 + 4\omega_o{}^2\tau_c{}^2)$$

Here η is the asymmetry parameter of the electric field gradient, the term in square brackets is the quadrupole coupling constant, $J(\omega_o)$ and $J(2\omega_o)$ are the spectral densities at the Larmor frequency and at twice that value, and τ_c is the rotational correlation time of the gradient vector. In O-D or C-D bonds the gradient of the electric field experienced by the deuterium nucleus is very close to the direction of the σ bond. In a first approximation, the rotational autocorrelation function of the O-D bond in DHO could describe properly the rotational dynamics of the molecule in the field. Therefore, T_1 depends only on the reorientational dynamics of the solvent and not on the average orientation. Simultaneous measurement of $\Delta\nu$ and T_1 allows testing for the two effects, dynamics and average orientation.

The difference in T_1 of HDO between both systems is about 30%. According to the theory of relaxation,[33] the rotational autocorrelation times should not be significantly different, suggesting that the differences in the rotational dynamics of the solvent molecules could not account for the experimental observation. Even more, assuming

extreme narrowing conditions, $\omega_o\tau_c << 1$, a reasonable assumption for water, T_1 should be proportional to the inverse of τ_c, therefore the correlation time in CsDAla should be even shorter than in TTAB, displaying a smaller quadrupole splitting. This is in opposition to the experimental observation. Therefore, reorientational dynamics is not responsible for the observed difference.

Then, the difference in splitting should arise either from a thicker anionic interface, able to accommodate more solvent molecules, or may be due to the existence of more oriented solvent molecules in the anionic interface. To discriminate between these two effects we performed classical mechanics simulations of both systems.

Molecular Dynamics. A unit cell was built containing two TTA^+ ions and one central decanol, both with the aliphatic chain in the fully extended 6-31G* minimum energy conformation. The unit cell was copied in the X and Y directions to generate a monolayer. This monolayer, containing 96 TTA^+ ions and 48 DeOH, was displaced 1.7 nm in the Z direction, copied, and rotated 180° around the Y-axis to generate the desired bilayer. This system was included in a rectangular box of dimensions 6.5 x 7.1 x 6.1 nm^3, with periodic boundary conditions in the three directions of space, containing 4192 SPC[17] water molecules, 288 NaCl and 192 Cl^- ions. The components of this bilayer are not centered along the Z axis of the box, but since there are periodic boundary conditions in all directions, this should not represent an inconvenience. The energy of this bilayer was minimized, to avoid bad contacts and overlaps, and 15 ns of trajectory were calculated using the (N, P, T) ensemble. A similar procedure to the one described was employed to assemble the CsDAla bilayer. The simulation included 120 alaninate ions, 60 decanol molecules, 3347 water molecules,[17] 120 cesium ions, and 38 KCl, all enclosed in a box of dimensions 6.0 x 4.6 x 6.6 nm^3, with periodic boundary conditions. After energy minimization, a 15 ns trajectory of the (N, P, T) ensemble was calculated.

All the information extracted from the trajectories was obtained from the last 10 ns of calculation, to be sure that the systems were completely equilibrated.

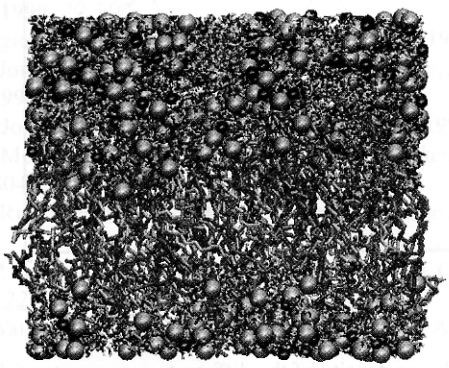

Fig. 2. Snapshot of the TTAC bilayer after 7 ns trajectory. TTA^+ is orange, DeOH grey, Cl^- light blue and Na^+ dark blue.

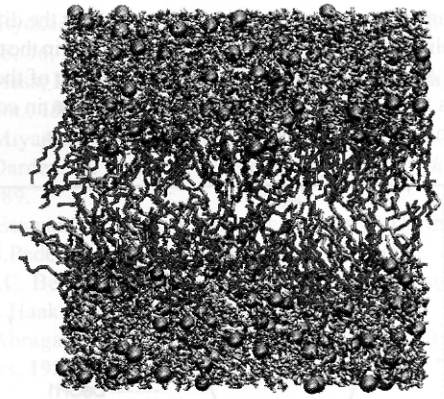

Fig. 3. Snapshot of the CsDAla bilayer after 7 ns of trajectory. $DAla^-$ is green, DeOH grey, Cs^+ pink, K^+ purple and Cl^- light blue.

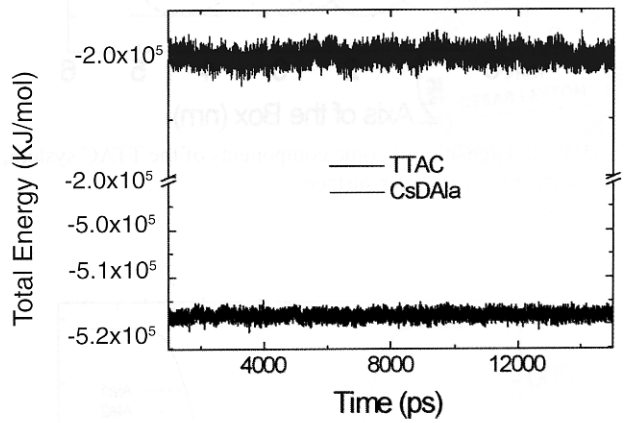

Fig. 4. Total energy of the studied systems vs. time. It can be estimated that fluctuations are about 1% in TTAC and 2% in CsDAla.

Figure 2 shows a picture of the TTAC bilayer and figure 3 is a snapshot of the CsDAla system, both equilibrated after a 7 ns trajectory. Figure 4 is a plot of the total energy as a function of time, for both bilayers. It shows that in the last 10 ns of trajectories the bilayers were completely equilibrated. The fluctuations in the energy are about 1% for TTAC and 2% for CsDAla. The different components of the energy were also examined, and all remained constant along the simulation. A visual inspection of the animation of the trajectories allows to conclude that the integrity of the bilayer structures remained unaltered during the complete simulation. Therefore, it is possible to obtain meaningful equilibrium statistical information about the systems.

Figures 5 and 6 are plots of the densities of TTA^+, $DAla^-$, DeOH and the solvent along the Z axis of the box for both systems. For a better representation of the results, each amphiphile is divided into three fragments. For DeOH the head group with the first two methylenes are the first fragment, the central hydrophobic region is the second fragment, and the last two carbon atoms of the chain are the third fragment; for TTA^+, the first fragment is the ammonium head group and the first methylene, the second is the central portion of the chain, and the third is the last two carbon atoms of the chain; for $DAla^-$ the first fragment is the complete amino acid including the carbonyl group, the second is the next nine carbons, and the third is the last two carbons of the chain. The plotted values correspond to the positions of the center of mass of each fragment.

Figures 5 and 6 clearly show that the bilayers are made of the amphiphilic ions and decanol, properly oriented along the Z axis of the

box. From the same figures it is possible to conclude that the differences in quadrupole splitting can not be attributed to differences in the thickness of the interface. According to these figures, the interface of the anionic aggregate seems to be thinner than the cationic interface, in contrast to the expected behavior if it was the origin of the difference.

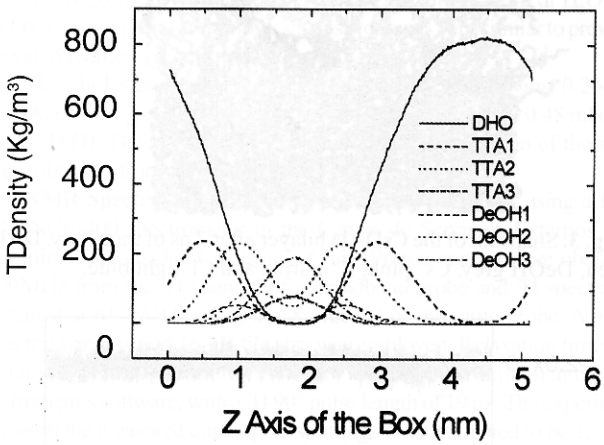

Fig. 5. Partial densities of some components of the TTAC system, along the normal to the bilayer surface.

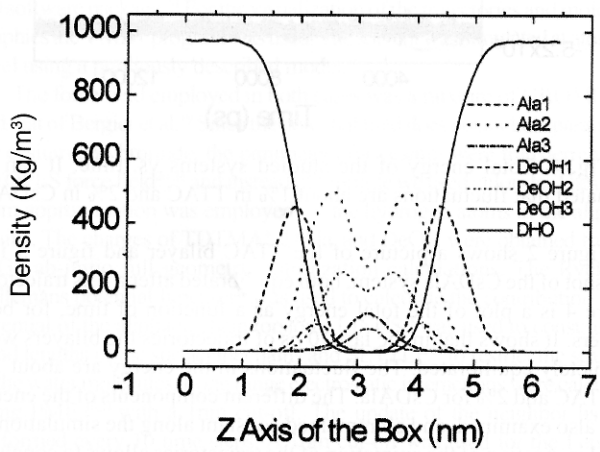

Fig. 6. Partial densities of some components of the CsDAla mesophase along the normal to the bilayer surface.

Since water possesses a very strong electric dipole moment, it is very likely that in the presence of a strong electric field it should become spontaneously oriented. To test for a preferential orientation of the solvent molecules at the interface due to the electric bilayer, we have calculated the charge density of the different components of the systems along the Z axis of the box. Figures 7 and 8 show the results of these calculations for TTAB and CsDAla, respectively. Both plots show the existence of an electrical bilayer formed by the charged head groups and the counter ions. However, it can be noticed that the polarization is significantly larger in the anionic aggregate compared with the cationic one. It is clearly seen that in CsDAla the counter ions K^+ and Cs^+ are strongly polarized. This is not observed for Cl^- in the TTAC mesophase. Perhaps the most important difference between both systems, and relevant to the purpose of this work, is the polarization of HDO at the interface. In fact, the HDO molecules in the anionic mesophase are more oriented, with the positive end of the dipole pointing toward the carboxylate groups of the alaninate, and the negative end pointing toward the positive counter ions, K^+ and Cs^+. The electric dipoles of the water molecules in the cationic mesophase are also oriented at the bilayer, with the positive end toward the counter ions and the negative end toward the ammonium, but in TTAC the charge density polarization is about one half as intense as in the anionic mesophase, evidencing a more randomly rotating solvent molecule. Therefore, the consequence of a more randomly rotating DHO molecule is a smaller quadrupole splitting, in agreement with the experiment.

Finally, we conclude that MD seems to provide an adequate representation of these systems. The observed difference between the quadrupole splitting of HDO, between the TTAB and CsDAla mesophases, can be mainly attributed to a preferential orientation of HDO at the anionic interface, due to the strong electric field induced by the electrical bilayer formed by the carboxylate groups of the alaninate and the counter ions. Differences in the thickness of the interface or restrictions to the reorientational dynamics of the solvent do not seem to explain the experimental observations.

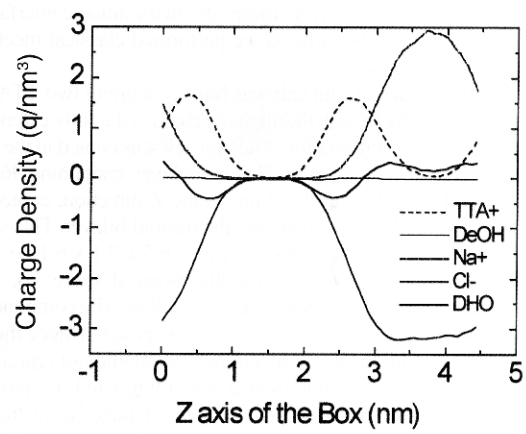

Fig. 7. Charge density of the components of the TTAB mesophase along the normal to the bilayer surface.

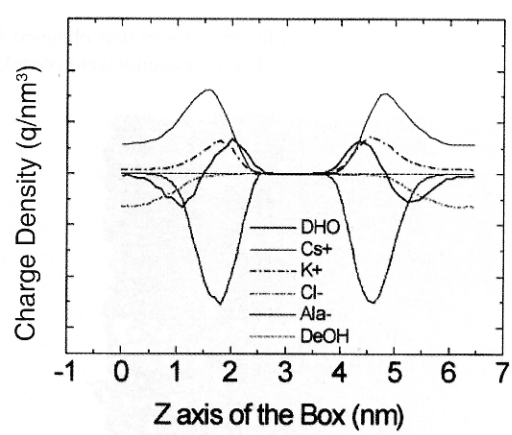

Fig. 8. Charge density of the different components of the CsDAla mesophase along the normal to the bilayer surface.

The authors are pleased to acknowledge financial assistance from Fondecyt, Project No. 1010211. H.A. and R.M. acknowledge Doctoral Fellowships from Conicyt.

REFERENCES

1. S. Balasubramanian and B. Bagchi, *J. Phys. Chem. B,* **2002,** *106,* 3668.
2. S. Balasubramanian and B. Bagchi, *J. Phys. Chem. B* **2001,** *105,* 12529.
3. N. Nandi.; K.Bhattacharyya and B.Bagchi, *Chem. Rev.* **2000**, *100*, 2013.
4. M. Benrraou; B.L. Bales; R. Zana; *J. Phys. Chem. B*, **2003**, *107*, 13432.
5. M. Fukuzaki; N.Miura; N.Sinyashikin; D. Kunita; S. Shiyoya; M.Haida and S. Mashimo, *J. Phys. Chem.* **1995**, *99*, 431.
6. D.P.Tieleman; D.van der Spoel; H.J.C.Berendsen; *J. Phys. Chem. B*, **2000**, *104*, 6380-6388.
7. X. Auvray; T.Perche; C.Petipas ; R.Anthore; M.J. Marti; I. Rico and A. Lattes; *Langmuir*, **1992**, *8*, 2671.
8. B. Weiss-López, C. Gamboa and A. S. Tracey, *Langmuir*, **1995**, *11*, 4844.
9. B. Weiss-López, D. Saldaño, R. Araya-Maturana and Consuelo Gamboa, *Langmuir*, **1997**, *13*, 7265.
10. B. Weiss-López, J. Vicencio and C. Gamboa, *Langmuir*, **1996**, *12*, 4324.
11. B. Weiss-López, G. Miño, R. Araya-Maturana and A.S. Tracey, *Langmuir*, **2000**, *16*, 4040.
12. B. Weiss-López, M. Azocar, R. Montecinos, B.K. Cassels, and Ramiro Araya-Maturana, *Langmuir*, **2001**, *17*, 6910.
13. A.S. Tracey and K.Radley; *J. Phys. Chem.*, **1984**, *88*, 6044.
14. *Gromacs User manual* V *3.0*, van der Spoel, D., van Buuren, A.R., Apol, E., Meulenhoff, P.J., Tieleman, D.P., Sijbers, A.L.T.M., Hess, B., Feenstra, K.A., Lindahl, E., van Drunen, R., and Berendsen, H.J.C., Department of Biophysical Chemistry, University of Groningen, Groningen, The Netherlands, **2001**.
15. W. Humphrey, A.Dalke; K.Schulten; *J. Mol. Graph.*, **1996**, *14*, 33.
16. H.J.C.Berendsen; J.P.M.Postma; W.F. van Gunstere,; J.Hermans; Interaction Models for Water in Relation to Protein Hydration. In *Intermolecular Forces*; Pullman, B., Ed.; Reidel: Dordrecht, The Netherlands, **1981**, 331.
17. W.F.Van Gunsteren; H.J.C.Berendsen; Gromos Software Package, Biomos, Nijenborgh 4, 9747AG, Groningen, The Netherlands.
18. W.F.Van Gunsteren; H.J.C.Berendsen; *Angew. Chem. Int. Ed. Engl.*,**1990**, *29*, 992.
19. O.Bergier; O.Edholm, and Jhaning, F.; *Biophys. J.*, **1997**, *72*, 2002.
20. W. L. Jorgensen, D. S. Maxwell, and J. Tirado-Rives; *J. Am. Chem. Soc.* **1996**, *118*, 11225.
21. W. L. Jorgensen and N. A. McDonald; *Theochem* **1998**, *424*, 145.
22. N. A. McDonald and W. L. Jorgensen, *J. Phys. Chem. B*, **1998**, *102*, 8049.
23. R. C. Rizzo and W. L. Jorgensen, *J. Am. Chem. Soc.*, **1999**, *121*, 4827.
24. M.L.P. Price, D. Ostrovsky, and W. L. Jorgensen, *J. Comp. Chem.*, **2001**, *22*, 1340.
25. E.K.Watkins and W. L. Jorgensen, *J. Phys. Chem.* A, **2001**, *105*, 4118.
26. G.A. Kaminski, R.A. Friesner, J. Tirado-Rives and W.L. Jorgensen, *J. Phys. Chem. B.* **2001**, *105*, 6474.
27. J.P.Ryckaert and A.Bellemans; *Faraday Discuss. Chem. Soc.*, **1978**, *66*, 95.
28. B. Hess; H Bekker; H.J.C. Berendsen and J.Fraaije; *J. Cmpt. Chem.*, **1997**, *18*, 1463.
29. S. Miyamoto and P.A. Kollman; *J. Comp. Chem.*, **1992**, *13*, 952.
30. T. Darden; D. York and L. Pedersen; *J. Chem. Phys*, **1993**, *98*, 10089.
31. U. Essmann; L. Perera; M.L. Berkowitz; T. Darden,; H. Lee and L.G.Pedersen; *J. Chem. Phys.*, **1995**, *103*, 8577.
32. H.J.C. Berendsen; J.P.M. Postma; W.F.van Gunsteren; A. Dinola; J.R. Haak; *J. Chem Phys.*, **1984**, *81*, 3684.
33. A. Abragam, *Principles of Nuclear Magnetism,* Oxford Clarendon Press, **1985**, p. 314.